Journal of Nepal Geological Society, 2023, Vol. 66, pp. 61–74
https://doi.org/10.3126/jngs.v66i01.57925

Geostatistics and inverse distance weighing (IDW) multivariate interpolation methods for regional geochemical stream sediment survey for base metal prospecting around Wapsa, Solukhumbu District, Nepal

Dharma Raj Khadka

Department of Mines and Geology, Lainchaur, Kathmandu, Nepal
Corresponding author's email: khadkadr@yahoo.com

ABSTRACT

A systematic regional geochemical stream sediment survey for base metals copper, lead, and zinc over an area of 200 sq.km was carried out around Wapsa in Solukhumbu District. 200 stream sediment samples were collected from active streams and analyzed them using atomic absorption spectrometry (AAS) method. All chemical analysis data were interpreted with geostatistical analysis and inverse distance weighing (IDW) multivariate interpolation method using the geographical information system (GIS). The results have shown consistency with geology, homogeneity, and mineralization in the area which is verified with significant copper anomaly over an old working area around Wapsa. The $\log_{10}$ transformed data of Cu, Pb, and Zn were used to estimate threshold and anomaly determination. The method is valid for regional geochemical stream sediment surveys for base metals prospecting.

Keywords: Geology, base metal prospecting, geo-statistics, IDW interpolation, anomaly detection

Received: 10 February 2023 **Accepted:** 07 June 2023

INTRODUCTION

The geochemical prospecting method involves systematic measurement of the chemical properties of natural materials (Carranza, 2009). A systematic stream sediment survey coverage for base metal exploration was active till 2004 in Nepal. It has covered many parts of the Lesser Himalaya. A number of geochemical anomalies were identified for Cu, Pb, and Zn in the survey areas. The mean ±2 standard deviation methods of statistical analysis were applied to ascertain the background, threshold, and anomaly of the concentration of base metals at 1:63,000 scale base maps (UN/MEDB, 1981).

Mineral exploration was conducted in a 16,000 sq. km area mostly covering central Nepal (UN/MEDP, 1981). The exploration was restricted to metallic mineral prospecting mainly for base metals. The main exploration hypothesis for the program was metallogenic province may coincide with the geological zonation of the Himalaya since the Tibetan Plateau has calc-alkaline intrusive, the Indus Suture zone has an ophiolite belt, the Tethys zone has unmetamorphosed fossiliferous self-sediments of the outer edge of the Indian plate. Higher Himalayan crystalline rocks are represented by strongly metamorphosed kynite sillimanite schists, marble, granite gneiss, and migmatites. The Lesser Himalaya is represented by shallow water clastics and carbonate beds thrusted and metamorphosed to a variable degree (UN/MEDP, 1981). A porphyry copper province in Tibetan Plateau, Cr-Ni province in Indus Suture Zone in which chromium in Afghanistan and copper in Pakistan ophiolites, Barite-fluorite province in Tethys sediments, mica-beryl pegmatite province in Higher Himalaya, similarly Cu, Pb, Zn province in the Lesser Himalaya and Uranium province in Siwaliks (UN/MEDP, 1981). Considering the base metal province in the Lesser Himalayan region four prospects were drilled out of 250 highly encouraging geochemical anomaly areas but no ore bodies have been proven and suggested as the economic deposit of copper and is likely to be found in Nepal (UN/MEDP, 1981). The assessment of the regional geochemical mapping resulted from the validity of the procedures and demonstrated to be an effective technique to eliminate ground of low mineral potential (UN/MEDP, 1981). The anomalous zones of copper and its showings, occurrences and deposits were compiled based on the available data driven by DMG (Talalov, 1972; UN/MEDP, 1981; UN/ESCAP with DMG, 1993; Joshi et al., 2004; Kaphle, 2020; this study) (Fig. 1).

Successively, a geochemical survey in the eastern parts of Nepal was partially covered during that UNDP project period (1975-1980). The northern part of central Nepal was covered partially in the following years by DMG (Fig.1). Similarly, parts of far-western Nepal were covered for base metal prospecting in the later periods (Joshi and Thapa, 1977; Kaphle, 2020, 1992, 1984, 1982; Kaphle and Khan, 1993; Khan, 1994, 1995, 1997; Jnawali and Amatya, 1993). The reconnaissance geochemical stream sediment survey results were also geostatistically interpreted for Cu, Pb, Zn anomalous categories of 2 to 4 in parts of Dailekh and Achham districts (Khadka, 2003). The findings of the base metal anomalies, showings, and old workings were compiled (Joshi et. al., 2004; Kaphle, 2020) (Fig. 1). The regional geochemical survey was mostly covered in far-western Nepal, some parts in Central and Western Nepal much of the LHS was completed by DMG except for some parts of mid-western Nepal (Fig. 1). A number of copper anomalous areas and their showings, occurrences and deposits were identified during the prospecting of base metals in Nepal (UN/MEDP, 1981; UN/ESCAPE with DMG, 1993; Joshi et. al., 2004; this study).

Classical statistical methods have been used for the delineation of anomalies from the background by plotting histograms and analysis, box plots, summation of mean, and standard

deviation coefficients and median (Gałuszk, 2007; Hawkes and Webb, 1962; Reimann et al. 2005; Stanley and Sinclair, 1989). Hosaaeininasab et al. (2018) applied the inverse distant weighting (IDW) and the concentration area (C-A) fractal methods for Fe, As, Mo, and Pb from 300 stream sediment samples from Janja region SE Iran. This area was gridded by 250×250 m resolution, and estimation of the unsampled area was carried out by the inverse distant squared weighting (IDW) method. Geochemical anomaly maps were generated and log-log plots of the cumulative frequency of elemental concentrations were constructed and also threshold values were obtained in which a good correlation between faults and elemental anomalies was established and concluded that most of the mineralization occurred along the faults. Anomalies should be assessed on the basis of magnitude, homogeneity, mineralization potential, rock type, erosional features, and sources of contamination (Haldar, 2018). The old workings and smelter slags, land-sliding of the mineralized zone, and fine suspended loads during the rainy period could have limitations in identifying correct anomalies (Carranza, 2009; Haldar, 2018).

This paper basically deals with the stream sediment survey for base metal prospecting and interpretation around Wapsa in Solukhumbu District, between latitude 27°30'00" to 27°35'00" N and longitude 86°40'00" to 87°00'00" E (topographic map Sheet No. 2786 07, 08) at 1:50,000 scale, covering over 200 sq. km. The field investigation work was under the annual regional geochemical survey for base metals and also a continuation of the regional geochemical survey under the DMG project in 2012 (Figs. 1, 2). The choice of the area is based on the existing old working Wapsa copper deposit which appeared to be sub-economic old workings. There are insufficient geological and stream sediment geochemical mapping within and its adjacent areas therefore, the IDW method of interpolation for anomaly detection of Cu, Pb, and Zn aided with classical geostatistical analysis for threshold computation to test with known Wapsa copper anomaly.

MATERIALS AND METHODS

Desk study

The available secondary data were collected from different sources and reviewed during the desk study. Almost all the available published literatures and unpublished reports of particular interest focusing on the Wapsa copper prospect were reviewed. The desk study also covers public library consultation, website data collection, etc.

Field study

Geological mapping: The field equipment consists of a geological hammer, Brunton compass, hand lens, measuring tapes, topographic maps, notebooks, scales, protractors, dilute HCl, and GPS. During geological field mapping standard methods were applied as per the basic geological mapping

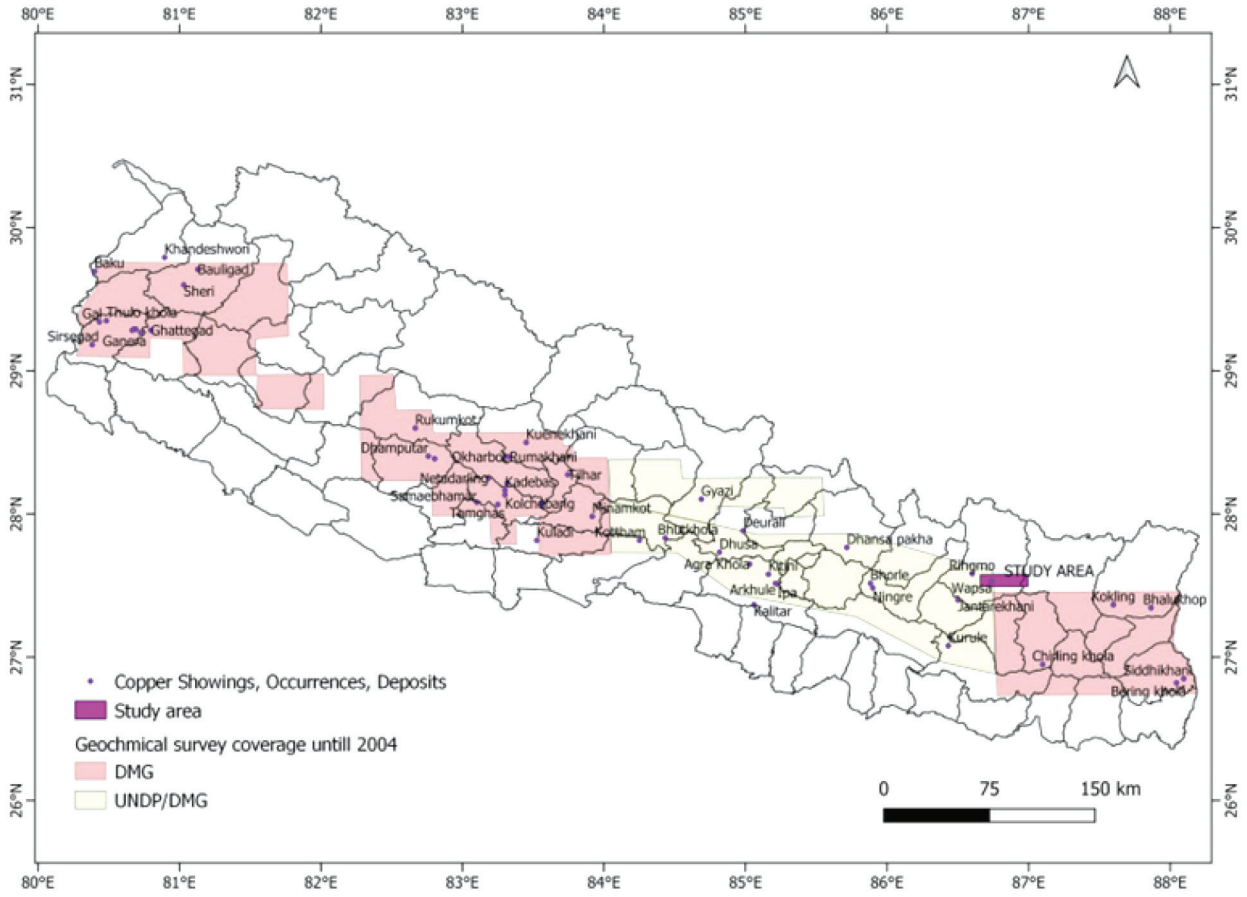

Fig. 1: Regional geochemical survey of Nepal and location of the study area (modified after UN/ESCAP with DMG 1993; UN/MEDP, 1981; Joshi et al., 2004; Kaphle, 2020; this study).

(Barnes, 2004). The topographical base maps at the scale of 1:50,000 were used mainly to locate the prospecting site and sampling points. The geological mapping and geochemical stream sediment sampling for base metal prospecting were performed simultaneously based on the ridge & spur and river section walkover survey. The lithological data and attitude of bedrock were measured by Brunton compass, and sampling sites/ points were marked with the help of topographic maps and GPS. The contacts between lithological units and bedrock outcrop mapping was partially supplemented with field observations. The collected data were plotted on the topographic map. The field photography was documented and the lithological units were identified. The field notebooks were maintained for geological and sampling information which is necessary for GIS application. The regional geological map was prepared at a scale of 1:50,000.

Heavy mineral concentrate (HC) sampling: The field materials also consist of a 2 mm sieve, large and small gold pans for panning the stream sediments, a can to collect samples, digging tools, sample bags, gloves, marker pen, notebook, and had-lens. The heavy concentrate sampling methods were followed as per the mineral exploration methods internationally as Britain, panned concentrate drainage sampling (NERC, 2001). The sampling density adopted was 1 sample/sq.km. The sampling method consists of collecting about four large pans of a sediment sample from selected sites, panning, standardization of the volume of sediment to be panned, the final volume of panned concentrate, 2 mm sieve concentrate, careful rubbing and shaking, washing concentrate with water for clay and organic matter until the water remains clear. Washing and panning of the samples were done in still water, near circular swirling motion of water, and frequent examination of the concentrate with a hand-lens. About 40 g HC samples from each sampling site were concentrated and packed them separately for lab study/ analysis. The site selection was considered to avoid sources of contamination, collecting samples from mineral trap areas such as behind large boulders and inside stream/ river bends. GPS location data were collected for each sampling site. The geological and structural homogeneity and contrast were considered for sampling (Carranza, 2009). A total of 27 HC samples were collected from the area.

Stream sediment sampling: The field materials consist of an additional sieve of 200 μm. The stream sediment sampling methods were followed as per the mineral exploration methods in Britain (NERC, 2000; Darnley, 1995) and the USA (Arendt, 1978). The sampling density was 1 sample/sq.km. About 500 g to 1 kg sediment samples (depending on the size of the sediment) from each sampling site were collected from the active stream bed below 10–20 cm from the surface just to avoid contamination. All samples were air dried under the sun, sieved through 200 μm sieve, and only minus 200 μm sized 25 to 40 g samples were packed in labelled sample bags for chemical analysis of base metals. The contamination was avoided for sampling, 50 m upstream of the roads and inhabitants and collapsed banks were considered for sampling. The geology

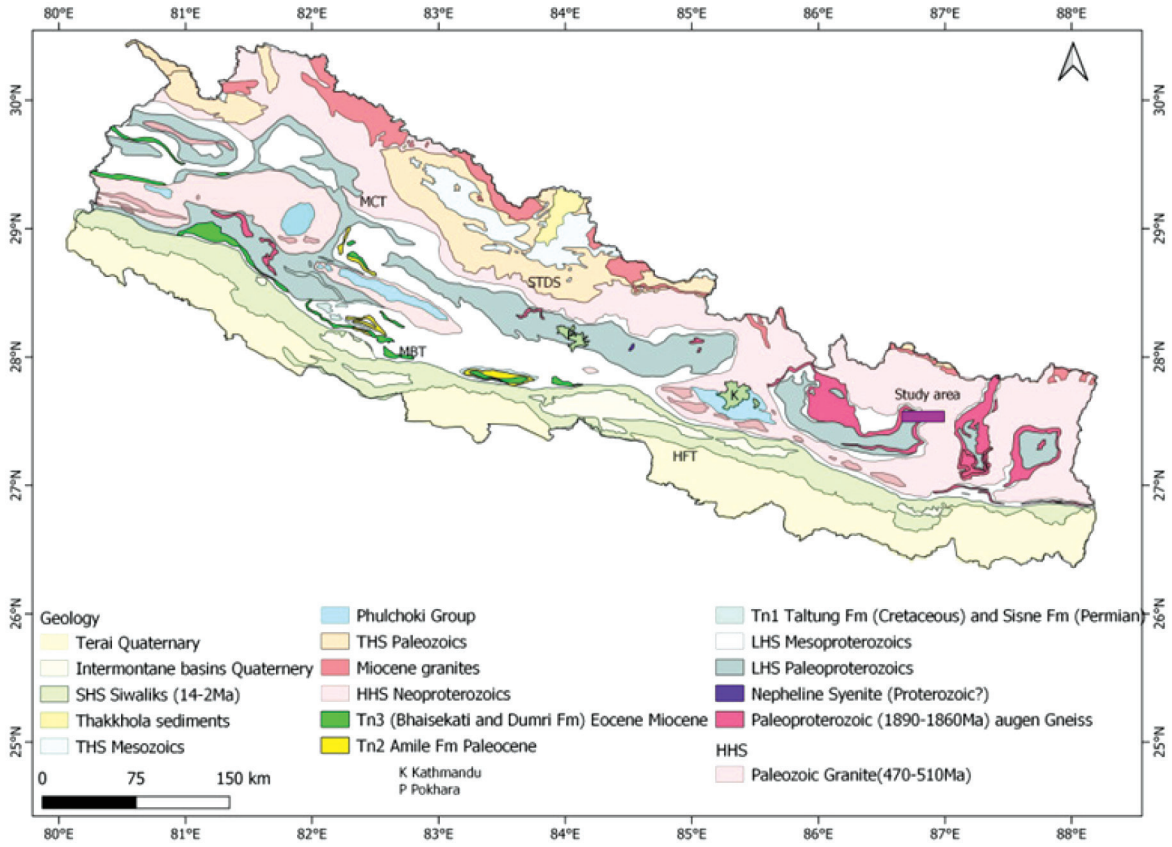

Fig. 2: Regional geological framework of Nepal (modified after Amatya and Jnawali, 1993; age data compiled after DeCelles et al., 2020).

of the catchment area and GPS data were collected at each sampling point. On average about 20 stream sediment samples were collected per day. None of the samples were collected from large rivers as it could have dilution effects. A total of 200 stream sediment samples were collected from 200 sq. km area.

Laboratory study

All the 200 stream sediment samples collected in the field were directly delivered to the chemical laboratory of DMG, for Cu, Pb, and Zn analysis in them. The atomic absorption spectrometry (AAS) method was employed for chemical analysis. Almost all the HC samples were also studied under the binocular microscope to know the heavy minerals present in the sediment derived from that particular catchment area.

Geostatistical methods of data interpretation

The statistical methods for data interpretation were carried out based on the standard practices and theoretical concepts of geostatistics (Carranza, 2009; Haldar, 2018; Zheng et. al., 2014). Basic equations 1–8 are generally used to interpret the geostatistical data.

where, minimum = Xmin (smallest) and maximum = Xmax

$$Range = Xmax - Xmin \quad (1)$$

(largest value)

$$\text{Mean} = \bar{X} = \frac{\sum_i^n Xi}{n} \quad (2)$$

$$\text{Standard error} = \frac{\sigma_x}{\sqrt{n}} \quad (3)$$

$$\text{Median} = \frac{(n+1)}{2} \quad (4)$$

Mode = value that occurs in a set of numbers or the highest frequency in grouped data or in a sample population

$\log_{10}$ = value of $\log_{10}$ is 1.

$$\text{Sample variance} = \sum_{i=1}^{n} \frac{(Xi-\bar{X})^2}{n-1} \quad (5)$$

$$\text{Standard Deviation} = \sigma = \sqrt{\frac{\sum_{i=1}^{n}(Xi-\bar{X})^2}{n}} \quad (6)$$

$$\text{Kurtosis} = \frac{\sum_{i=1}^{n}(Xi-\bar{X})^4}{n\sigma^4} \quad (7)$$

$$\text{Skewness} = \frac{\sum_{i=1}^{n}(Xi-\bar{X})^3}{(n-1)\sigma^3} \quad (8)$$

Log-normal distribution: Log-normal distribution is commonly used to model variables that are strictly positive and have a skewed distribution. It considers taking logarithms of data to transform into a normally distributed form. The geochemical data exhibit log-normal distribution since they are the result of various processes. This is used to describe the distribution of mineral resources in terms of grade and size.

Correlation coefficient (R): It is the ratio of covariance of two variables and the product of their standard deviation. Its value ranges from +1 to -1 SD), sample variance, kurtosis, skewness, range, minimum, maximum, 25th percentile, 75th percentile and 95th percentile for both natural samples and $\log_{10}$ transformed Cu, Pb, Zn values (Haldar, 2018; Zheng et. al., 2014). The data analysis consists of maxima and minima for bin categorization and frequency assignment. The frequency versus natural sample values and logarithmic values were plotted in histograms. The threshold value was calculated for Cu, Pb, Zn (Carranza, 2009) separately. The mean ± 2SD method was also applied to stream sediment data to delineate copper anomaly in Zhunuo area of southern Tibet (Zheng et al., 2014).

Inverse distance weighting (IDW) interpolation

The inverse distance weighting (IDW) method as a deterministic for multivariate interpolation with known nearby points was used to estimate the value of unknown points by the weighted average of the values of the known points using GIS. The concept of IDW is given in Equation 9 (Shepard, 1968).

$$Z_p = \frac{\sum_{i=1}^{n}\left(\frac{Zi}{di^p}\right)}{\sum_{i=1}^{n}\frac{1}{di^p}} \quad (9)$$

where, Zi= known point, di= distance between unknown point to known point, Zp= unknown point.

The inverse distance weighting (IDW) multivariate interpolation method was used for natural samples for anomaly detection. The geostatistical parameters were calculated to assign Bins and frequency of data sets. The $\log_{10}$ transformed data were used to calculate threshold. The data distribution maps were interpreted with respect to geological control, homogeneity, and mineral concentration.

Data interpretation

The geological map, stream sediment sample location map and Cu, Pb, and Zn anomaly maps were prepared by using GIS. The inverse distance weighting (IDW) interpolation method was applied to detect anomalies of Cu, Pb, and Zn. The Cu, Pb, and Zn IDW interpolated distribution maps were generated and interpreted for natural samples.

GEOLOGY

Regional geology

The continent-continent collision between the Indian and Eurasian plates resulted in the Himalayan Orogen (Gansser, 1964). Indus Tsangpo Suture (ITS) collision zone forms between the Indian and Eurasian plates from Myanmar to Afghanistan (Hodge, 2000). Nepal Himalaya is the central sector of the Himalayan Orogen. The geological map of Nepal (1:1,000,000 scale) was compiled by Amatya and Jnawali and published by DMG, in 1993 (Fig. 2). The Tethys Himalayan Sequence (THS) consists of Paleozoic to Eocene Indian continental margin sediments (Garzanti, 1991). The South Tibetan Detachment System (STDS) separates high-grade metamorphic rocks of the Greater Himalayan Sequence (GHS) and THS (Burg, 1984). The GHS consists of high-grade crystalline rocks and meta-igneous rocks (Gansser, 1964; Stocklin, 1980; Le Fort, 1975). The GHS has been considered to be of Neoproterozoic or younger depositional age (Parrish and Hodge, 1996; DeCelles et al., 2020). The Lesser Himalayan Sequence (LHS)

consists of rocks of lower greenschist to amphibolite facies of metasedimentary rocks deposited in the Indian passive margin (Gansser, 1964). The age of the older LHS has been considered to be of Paleo-Meso Proterozoic (Martin, 2017; Brookfield, 1993; DeCelles et al., 2020). The Main Central Thrust (MCT) separates GHS and LHS (Martin, 2016). The late Paleozoic to Paleocene sedimentary units conformably overlie the older metasedimentary units of LHS (Stöcklin, 1980; Valdiya, 1980; Sakai, 1987; Dhital, 2015). The Eocene strata of Himalaya foreland basin deposits unconformably overlie Paleozoic to Paleocene sedimentary units (Decelles, 1998a, 2020). The Sub-Himalayan Sequence is dominated by Siwalik molasses sediments and separates with LHS by Main Boundary Thrust (MBT) (Decelles, 1998b; Dhital, 2015). The Indo-Gangatic sediments and Sub-Himalayan Sequence (Siwaliks) are separated by Main Frontal Thrust (MFT) (Decelles et al., 1998b; Dhital, 2015). The LHS has Pre-Himalayan and a Neo-Himalayan prograde inverted metamorphism whereas the GHS has kyanite-grade prograde metamorphism overprinted by Neo-Himalayan retrograde metamorphism in which the LHS and GHS have undergone late-stage retrogration during exhumation (Paudel and Arita, 2000). A number of Lesser Himalayan granitic bodies of Ordovician age (Einfalt et al., 1993; Beckinsale in Mitchel, 1981) have been mapped in the crystallines of the Mahabharat Range (Shrestha, 1984; Upreti, 1999; Kaphle, 1992).

The rocks occurring within the Seti Formation are considered to be equivalent to Kuncha Formation (Shrestha, 1984; Upreti, 1999; DeCelles, 2001, 2020; Pearson and DeCelles, 2005; Larson and Godin, 2009). This unit comprises the lowermost part of the LHS (Le Fort and Rai, 1999; Sakai, 2013). It consists of mylonitic, quartz-alkali feldspar-plagioclase-muscovite-biotite bearing orthogneisses (Ishida, 1969; Schelling, 1992; Larson, 2016, 2017) with granitic protoliths (Schelling, 1992; Larson, 2017). The orthogneiss is variably referred to as the Ulleri gneiss (Le Fort and Rai, 1999; Goscombe, 2006, Liu et al., 2022), Melung (Ishida, 1969), Melung-Salleri (Schelling, 1992), Phaplu (Jessup, 2006), or Num (Goscombe, 2000) Formation. These are also named by other local names in other parts of the country. They have intrusive relations with the host rocks of the Kuncha Formation (Larson, 2017). They were deposited in the Paleoproterozoic time (Martin, 2005; DeCelles, 2020). These rocks of the Kuncha Formation have been interpreted to reflect deposition in a rifted or passive margin (Brookfield, 1993; Sakai, 2013), or arc setting (Kohn, 2010). Larson (2019) concluded that the rocks of the Kuncha Formation were deposited in the Paleoproterozoic and have within-plate, A-type affinities, and generation in a rifted margin, and are compatible with an open boundary for present-day northern India in the Paleoproterozoic. Liu et al. (2022) studied anataxis in the MCTZ in Arun Valley, eastern Nepal. They concluded that a series of deformed rocks, including migmatites, gneisses, and leucosomes are found across the MCT in which the protolith boundary between the GHS and LHS has been recognized on the basis of Sr–Nd isotopes with εNd(0) of -16.7 to -8.0 for the GHS and -31.2 to -23.9 for the LHS. Moreover, based on the Zircon U–Pb geochronology, they suggested that partial melting (35–13 Ma) occurred in the MCTZ. Based on the zircon geochemical results, they suggested that hydrous meta-sediments from the LHS were progressively accreted to the base of the GHS, resulting in hydration melting of both the GHS and LHS assisted by MCT. The timing of activity of the MCT was constrained to 25–13 Ma, with the movement of the South Tibetan Detachment System. They also concluded that the thickened Himalayan crust was heated from the middle to late Eocene, and widespread anatexis occurred during the Oligocene to middle Miocene, forming a large-scale melt channel. Furthermore, with the cooling of the melt channel, duplexing has gradually operated since the middle to late Miocene in the shallow crust. The present study area is a northern part of the LHS and the southernmost basal part of GHS, structurally separated by Main Central Thrust (MCT) in some parts of Solukhumbu district, Nepal (Figs. 1, 2).

Geology of the study area around Wapsa in Solukhumbhu

Lesser Himalaya Sequence (LHS): The Lesser Himalaya Sequence is represented by Seti Formation equivalent to the Kuncha Formation (Shrestha, 1984, Upreti, 1999) and Benighat Slates in the study area (Stocklin, 1980) (Fig. 3). The Seti Formation consists of green chloritic schist, garnet biotite schist, and quartzite. These rocks are variably cropping out in the western part of the study area around Dudh Koshi River, Wapsa, Khastap, Chhechewa, Leldum, the southern part of Inkhu Khola and Sotan areas. The outcrops have medium to thick-bedded magnetite-bearing quartzite inter-banded with thinly foliated chloritic and biotitic schists. Seriticic schist and quartzite are dominant in the Sotan areas. The Dudhkoshi anticline runs almost NS in the western part of the Wapsa area. The attitude of beds is moderately dipping due NE and SW in the Wapsa area and in other parts with NE dipping. The orthogneiss intruded into the upper part of the formation is known as Ulleri augen gneiss (Lefort and Rai, 1999; Sakai, 2013). It crops out in the upper parts of Inkhu Khola, Khiraule, Dhapkharka, Juge, and the lower part of the Hongu Khola areas within the study area. The foliation is more or less parallel to the overlying and underlying country rocks. The porphyroblastic augen gneiss is intruded within the mica schists developing K-feldspar augens and is described as Melung Salleri orthogneiss (Larsen, 2017) equivalent to Ulleri orthogneiss (Sakai, 2013). The age of the orthogneiss is 1796± 6Ma (Larsen, 2017). The metabasites, metagabbro, metadolerite rocks are intercalated within the meta-sediments of the Kuncha Formation (Stöcklin, 1980; Larsen, 2017). The black carbonaceous pelitic schists inter-banded with meta-sandstone and marble is conformably overlying Seti Formation known as Benighat Slates in the area (Fig. 3). The upper part consists of thin beds of graphitic schists around Chheskum. They are cropping out in Chheskum, Hongu Khola, Phulpati Khola, and Surke areas (Fig. 3). The foliation is moderately dipping mostly due northeast (Fig. 3). The age of these units of LHS is considered to be Paleo- to Meso-Proterozoic (Martin, 2017). The lithological units of the study area are given in Table 1.

Higher Himalaya Sequence (HHS): The Higher Himalaya is represented by Formation I paragneiss, kyanite schists, and quartzite in the study area around the upper reaches of Hongu Khola, Bokswar, and Gurasekharka. It is the lower unit of HHS (Le Fort, 1975). The foliation of the beds is mostly dipping due

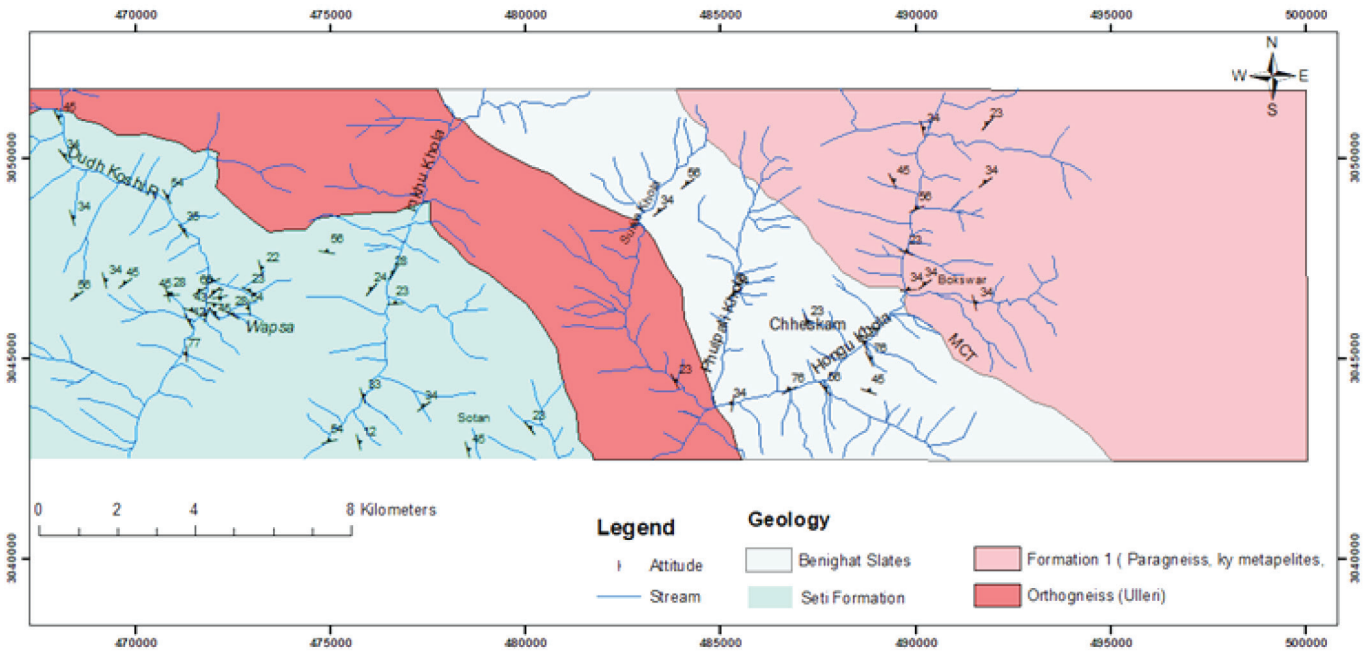

Fig. 3: Geological map of the study area around Wapsa in Solukhumbu district.

Table 1: Lithological units of the study area around Wapsa in Solukhumbu.

Sequences	Formation	Lithology	Age
Higher Himalaya Sequence (HHS)	Formation I	Paragneiss, kynite schist and quartzite	Neo-Proterozoic (Parrish and Hodge,1996)
---------- Main Central Thrust (MCT) ----------			
Lesser Himalaya Sequence (LHS)	Benighat Slates	Pelitic schist, metasandstone, marble, graphitic schist	Paleo to Meso-Proterozoic (Martin, 2017)
	Seti Formation	Ulleri Orthogneiss Green chloritic schist, garnet-biotite schist, quartzite	

NE. The age of the unit is considered to be of Neo-Proterozoic (Parrish and Hodge, 1996). It is a part of the Makalu-Barun Conservation area (Fig. 3, Table 1).

The rocks of LHS and HHS are separated by a very prominent Main Central Thrust (MCT), which is a sheared zone in the upper part of the Benighat Slates with graphitic and garnet schists and the Lower part of Formation 'I' kyanite schists and gneisses (Fig. 3).

WAPSA COPPER PROSPECT

The Wapsa copper prospect area is the westernmost small part of the study area (Figs. 1, 3, 4a,b). The Wapsa copper prospect corresponds to the schists and quartzites of Seti Formation of LHS. It had been investigated by Ranjitkar (1976) for the mineral economics of Wapsa Khani. Chhetri (1977) carried out channel sampling in Wapsa Audit No. 6. Shrestha (1978) investigated copper prospects with core drilling. Bhandari (1978) concluded the drilling results of drill holes UNDDH-18, 19, and 20. Shrestha and Bajracharya (1979) carried out IP and Magnetic survey. Similarly, Shrestha (1980) investigated the prospect with the second phase of core drilling. All these exploration works conducted by UN/ MEDP have confirmed that there exists a stratiform copper mineralized band of about 300m long, and mineralized body thickness varies from 2–3.5 m, with a grade ranges from 0.8 to 3% Cu and 2.4 million tons of copper ore deposit (UN/ MEDP, 1981) (Fig. 4a,b).

In Wapsa, structurally, the Dudhkoshi anticline passes through the Yasuka area as shown by the attitude of beds (Fig. 4a). Wapsa copper prospect is situated on the spur between the Rue and Guye Khola on the left flank of Dudh Kosi (Fig. 4a) and the area is mainly represented by quartz chlorite schist and quartzites. This copper prospect had been assessed by geochemical and geophysical surveys as well as with many trenches and 3 drill holes e.g. UNDDH-18, UNDDH-19, and UNDDH-20 by core drilling (UN/MEDP, 1981). All these works were able to trace a 20 m thick mineralized zone, Old working audits 1–7 from where the copper ore was extracted in the past. The main minerals identified are pyrite, chalcopyrite, bornite, covellite, and pyrrhotite in the ore samples as well as in heavy concentrate samples with magnetite and few garnet grains (Fig. 4a). Rest of the heavy concentrate samples from

other parts of the area consists of magnetite, garnet, zircon, rutile and few ilmenite (Fig. 4b).

The Wapsa copper deposit lies in a highly disturbed terrain due to old landslides created possibly due to haphazard mining activities in the past without any technical knowhow (Fig. 5a). A number of copper old working audits and pits were excavated to mine copper ore on the right bank of the Dudh Koshi River nearby Yasuka which is the right side of the ridge of Dudh Koshi River adjacent to the Wapsa. In almost all copper old workings malachite staining can be seen mainly in schists (Fig. 5c,f) at Yasuka. In the past, all mining activities were performed by applying local indigenous technology with a view to excavating copper ore and extracting copper metal. The drilling data ie core samples show that the ore body lies within 30–50 m depth from the surface (UN/ ESCAPE with DMG, 1993). The sulphide ore mostly consists of chalcopyrite (Fig. 5b) and a few associations of pyrite, arsenopyrite, and pyrrhotite. The old working copper slags are scattered around Olympic School (Fig. 5d). Some sulphide bearing quartzite can be seen around Audit-6 (Fig. 5e). Study of heavy mineral concentrate samples (HC-1 to HC-5) shows that there are nonmagnetic minerals like pyrite, chalcopyrite, garnet, rutile, and zircon. The stream sediment samples analyzed for copper content shows a high concentration (423 ppm Cu) in this Wapsa area (Fig. 4a, b).

GEOCHEMICAL STREAM SEDIMENT SURVEY

A total of 200 stream sediment samples (with sample density 1 sample per sq.km) were collected from the streams and their tributaries in the investigated area covering 200 sq.km. Wet samples were sun-dried and sieved through 200 µm mesh sieve. All these samples were supplied to the chemical laboratory of DMG for chemical analysis for Cu, Pb, and Zn. All the analytical data were treated statistically and interpreted to obtain the various geochemical parameters like background value, threshold value, anomalous value, and high anomalous values. Histograms and cumulative frequency curves were also plotted to verify the values. The background is the normal concentration of an element in non-mineralized earth material, whereas the threshold is the upper limit of the range of background values, and the concentration greater than the threshold is anomalous in which the threshold method is a standard technique to quantify geochemical data (Carranza, 2008; Sinclair, 1974). Classical geostatistical methods were applied to calculate the threshold considering the terrain geologically consists of pelitic protoliths with subordinate psammites. The sediment data were collected from LHS Schists and quartzites hosts and terrain has been taken as a single window for geochemical data processing.

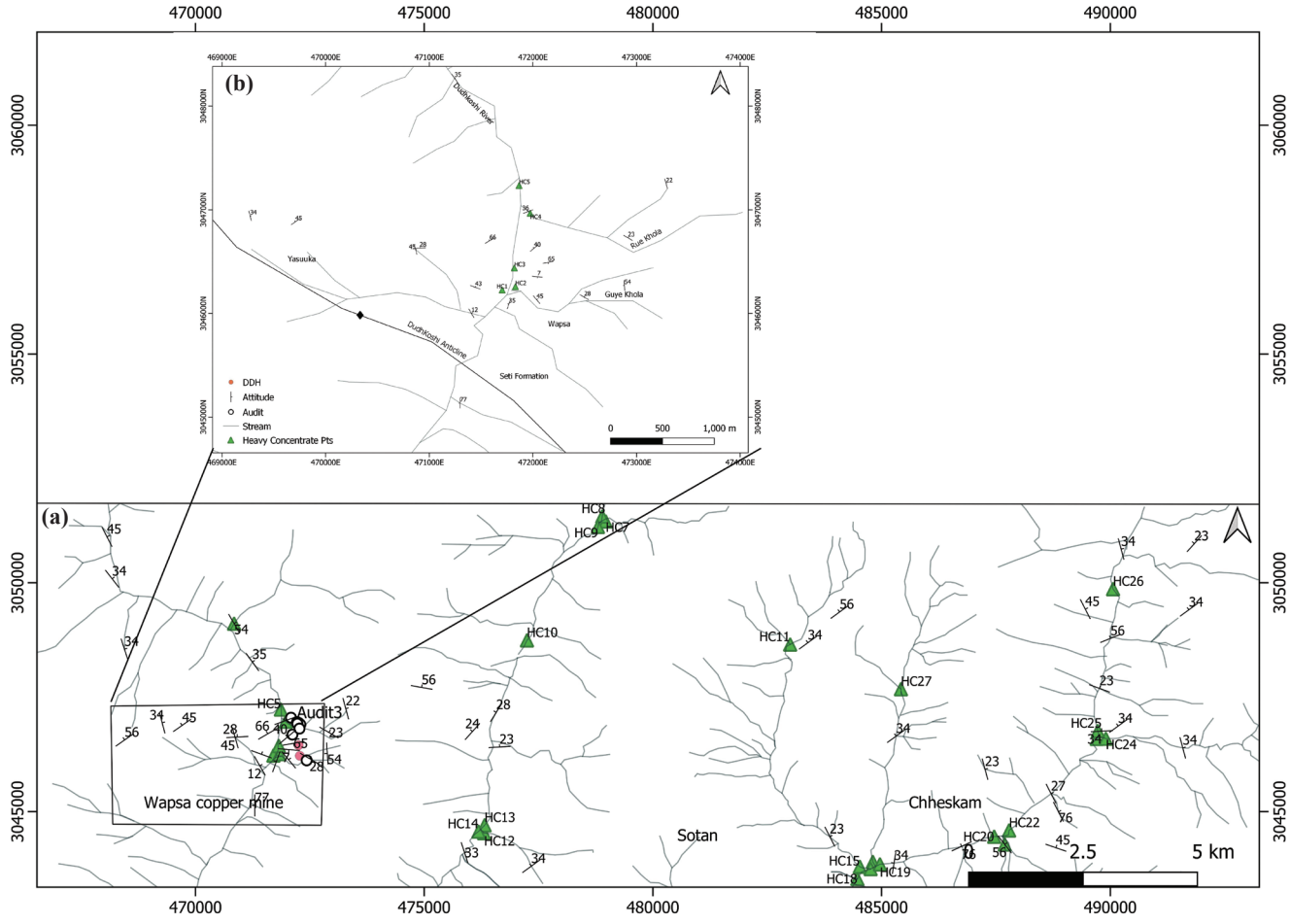

Fig. 4: (a) Wapsa copper prospect, the western part of the study area (modified after UN/MEDP, 1981; this study 2012), (b) heavy concentrate sampling locations in the study area, Wapsa mine area location shown in the inset.

Geostatistics

The 200 stream sediment samples analyzed for Cu, Pb, and Zn were statistically treated and calculated for mean, standard deviation, median, mode, sample variance, kurtosis, skewness, range, minimum, maximum, 25th percentile, 75th percentile and 95th percentile for natural samples (Table 2). The minimum and maximum values of Cu, Pb, and Zn were taken to assign bins for the frequency of samples. These values were plotted for Cu, Pb, and Zn against frequency. The natural samples show positively skewed histograms (Figs. 6a, c, e). All samples were transformed to $\log_{10}$ (Table 2). The minima and maxima of $\log_{10}$ were taken into consideration for bins assignment for the frequency determination of samples. The $\log_{10}$ values of Cu, Pb, and Zn were plotted against frequency. The histograms show that the Cu, Pb, and Zn values have a normal distribution (Figs. 6b, d, f). The mean and standard deviation values of the antilog were taken into consideration for threshold value computation for Cu, Pb, and Zn to analyze the anomaly pattern of the area in IDW interpolation (Table 3). The correlation coefficient for Cu, Pb, and Zn was calculated and transformed to R i.e. correlation coefficient for Cu-Pb, Cu-Zn, and Pb-Zn. The data shows that R for Cu-Pb is 0.38, Cu-Zn is 0.18 and Pb-Zn is 0.17 (Fig. 7a,b).

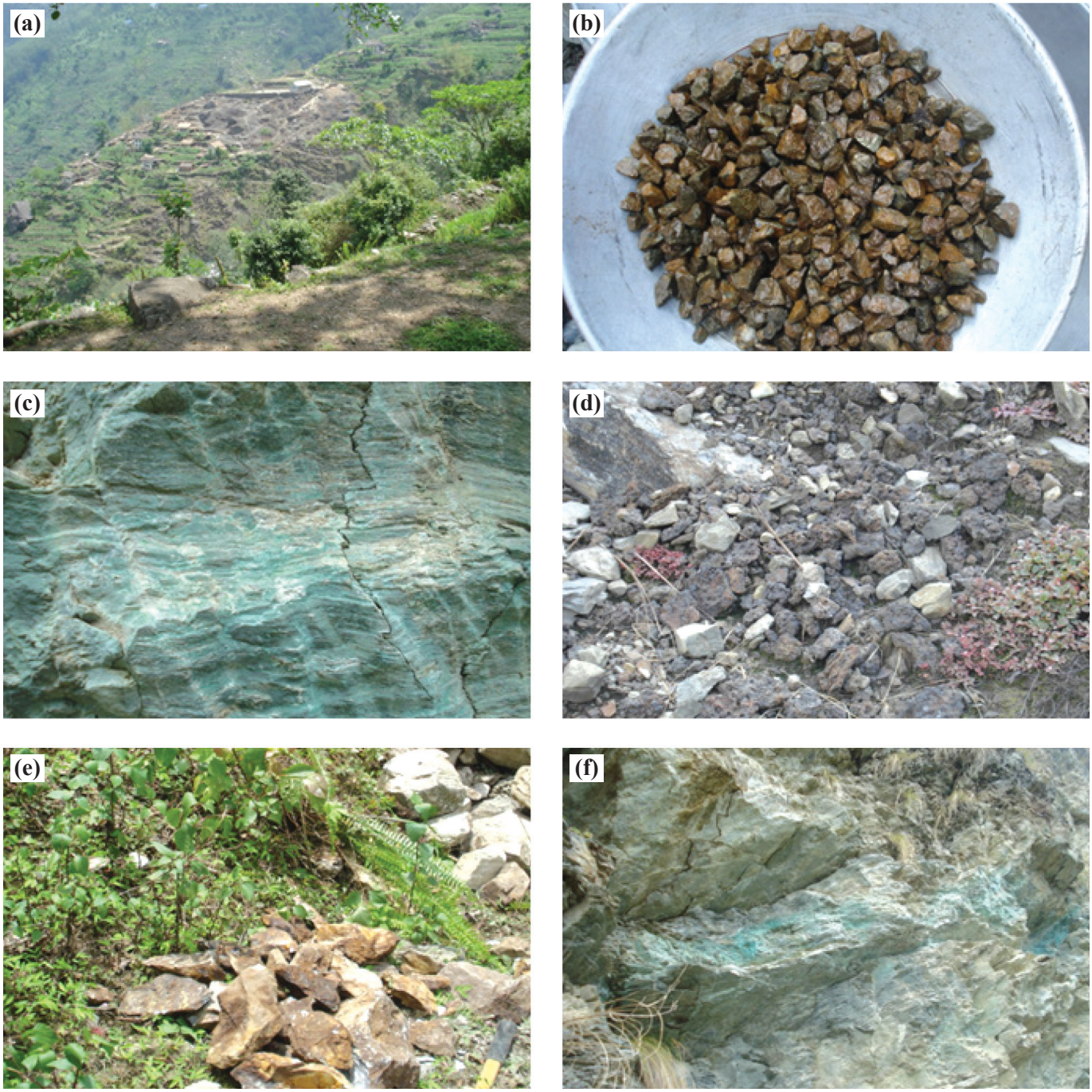

Fig. 5: (a) Wapsa copper deposit area, (b) primary concentrate of sulphide ores Wapsa, (c) and (f) malachite staining on schists in Yasuka area, (d) copper slag Wapsa, (e) sulphide ore bearing quartzite from Audit-6.

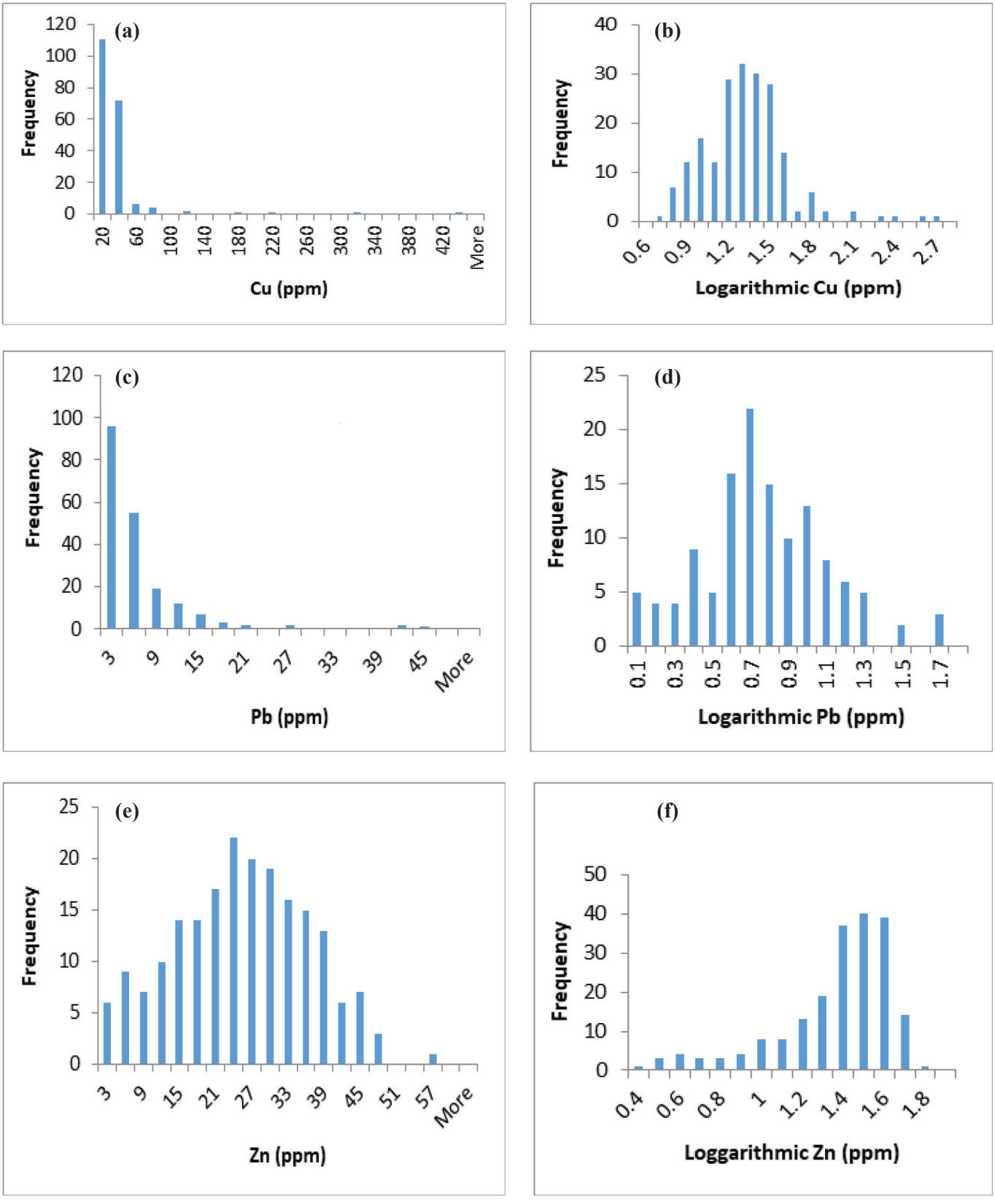

Fig. 6: Histograms of Cu, Pb, and Zn for natural samples (a, c, e) and $\log_{10}$ transformed (b, d, f).

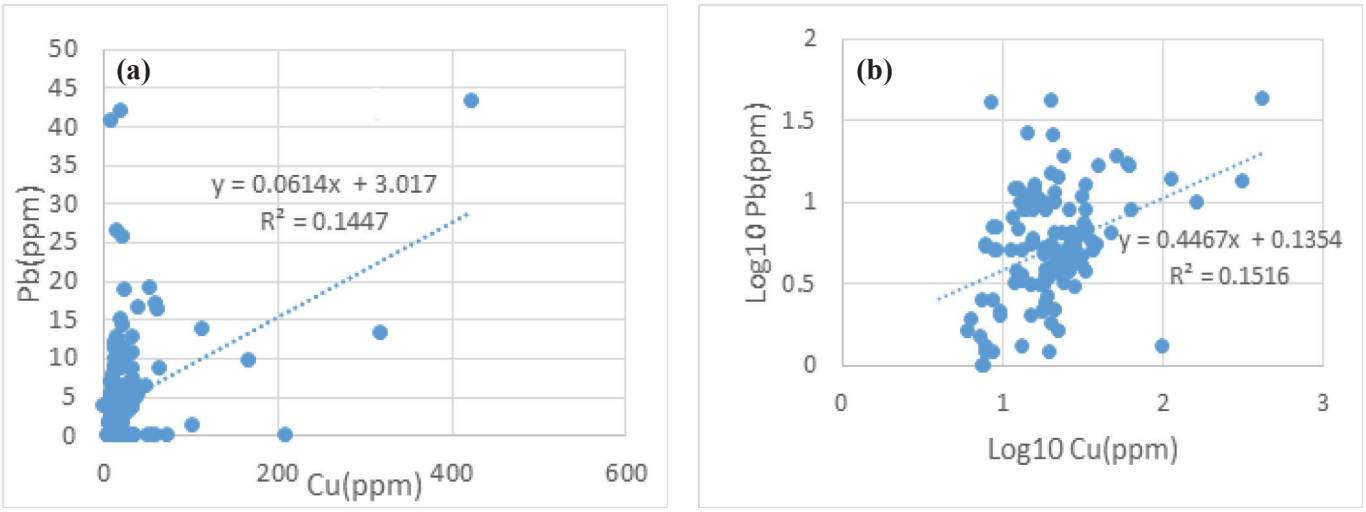

Log10	R^2	R	Natural	R^2	R
Cu-Pb	0.1516	0.389358	Cu-Pb	0.1447	0.380395
Cu-Zn	0.0048	0.069282	Cu-Zn	0.0334	0.182757
Pb-Zn	0.0342	0.184932	Pb-Zn	0.029	0.170294

Fig. 7: Correlation coefficient (R) for (a) natural samples, (b) $\log_{10}$ transformed data.

Table 2: Statistical parameters.

Natural samples	Cu	Pb	Zn	Log_{10} Cu	Log_{10} Pb	Log_{10} Zn
Total No. of samples	**200**	**200**	**200**	**200**	**200**	**200**
Mean	26.39	4.63	23.80	1.28	0.72	1.31
Standard error	2.95	0.48	0.80	0.02	0.03	0.02
Median	18.50	3.20	24.30	1.27	0.70	1.39
Mode	22.00	0.00	17.40	1.34	0.68	1.24
Standard deviation (SD)	41.61	6.71	11.26	0.30	0.34	0.28
Sample variance	1731.25	45.07	126.82	0.09	0.11	0.08
Kurtosis	55.34	13.76	-0.50	3.47	0.23	1.86
Skewness	6.88	3.18	-0.04	1.10	0.21	-1.42
Range	423.40	43.30	55.90	2.02	1.64	1.43
Minimum	0.00	0.00	0.00	0.60	0.00	0.32
Maximum	423.40	43.30	55.90	2.63	1.64	1.75
Sum	5250.70	920.50	4736.00	252.67	91.72	258.71
25th percentile	12.6	0	16.8			
75th percentile	26.5	6.0	32.4			
95th percentile	60.2	16.4	42.8			

Table 3: Threshold computation.

Ores	Natural mean	Threshold	Antilog mean	Threshold	95th percentile
	$\overline{X}$	$\overline{X}+2SD$	$\overline{X}$	$\overline{X}+2SD$	
Cu	26.39	109.61	18.88	22.88	60.2
Pb	4.63	18.05	5.27	9.63	16.4
Zn	23.8	46.32	20.57	24.37	42.8

Inverse distance weighing (IDW) multivariate interpolation

The normal stream sediment sample analytical results/ data are plotted with the Inverse Distance Weighing method of interpolation for natural data interpretation. The logarithmic values for the Cu, Pb, and Zn were used to present the background and threshold taking the antilog of the calculated data. The Cu mean value is 18.88 ppm which is considered to be the background value for copper and $\bar{X}$+2SD threshold is 22.88 ppm. The copper values greater than 23 ppm are considered anomalous. Based on the interpolation pattern of copper values, the Wapsa area has high copper anomaly over a significant area. The other parts of the sampled area show anomalous values in Bhuwa Khola and Hongu Khola tributaries and the Sotan area as shown in Figure 8.

The Pb mean value is 5.27 ppm and considered the background value for lead, and the $\bar{X}$+2SD threshold is 9.63 ppm. The lead values greater than 10 ppm are considered anomalous. Based on the interpolation pattern of lead values, Wapsa area has a lead anomaly. The other parts of the sampled area show anomalous values in Bhuwa Khola tributaries as shown in Figure 9.

The Zn mean value is 20.57 ppm and considered the background value for zinc, and the $\bar{X}$+2SD threshold is 24.37 ppm. The zinc values greater than 25 ppm are considered anomalous. Based on the interpolation pattern of zinc values, the Wapsa area has a zinc anomaly. The other parts of the sampled area show anomalous values in the Sotan area and Bhuwa Khola tributaries as shown in Figure 10.

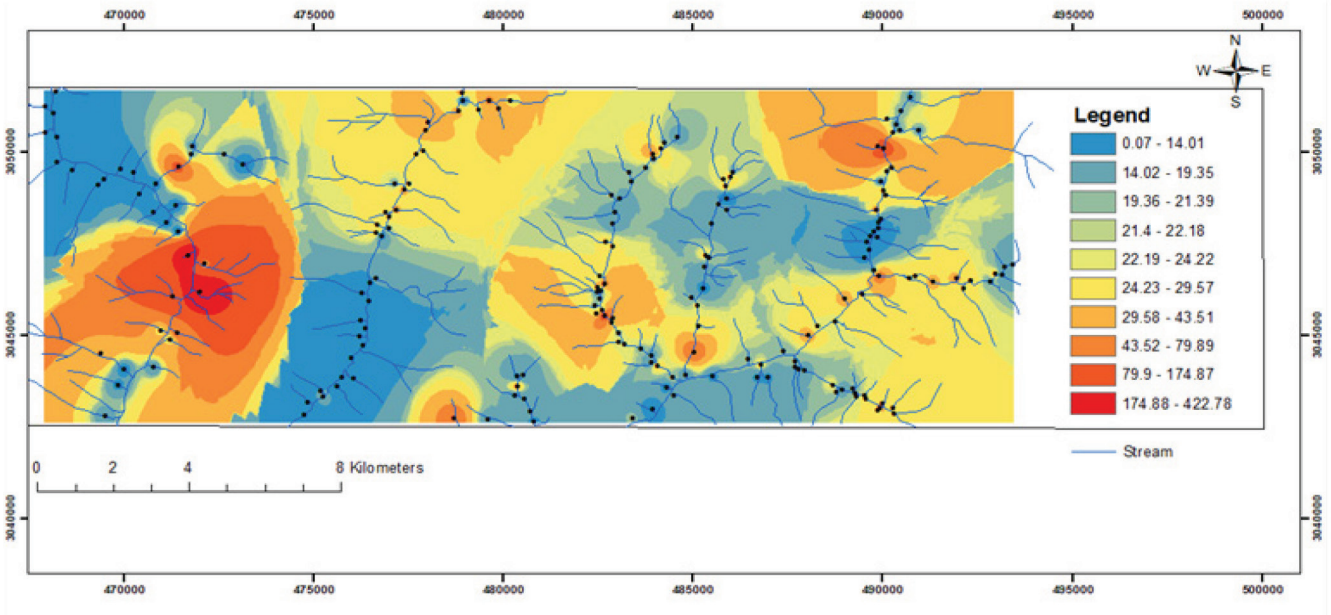

Fig. 8: Cu (ppm) distribution map of the study area.

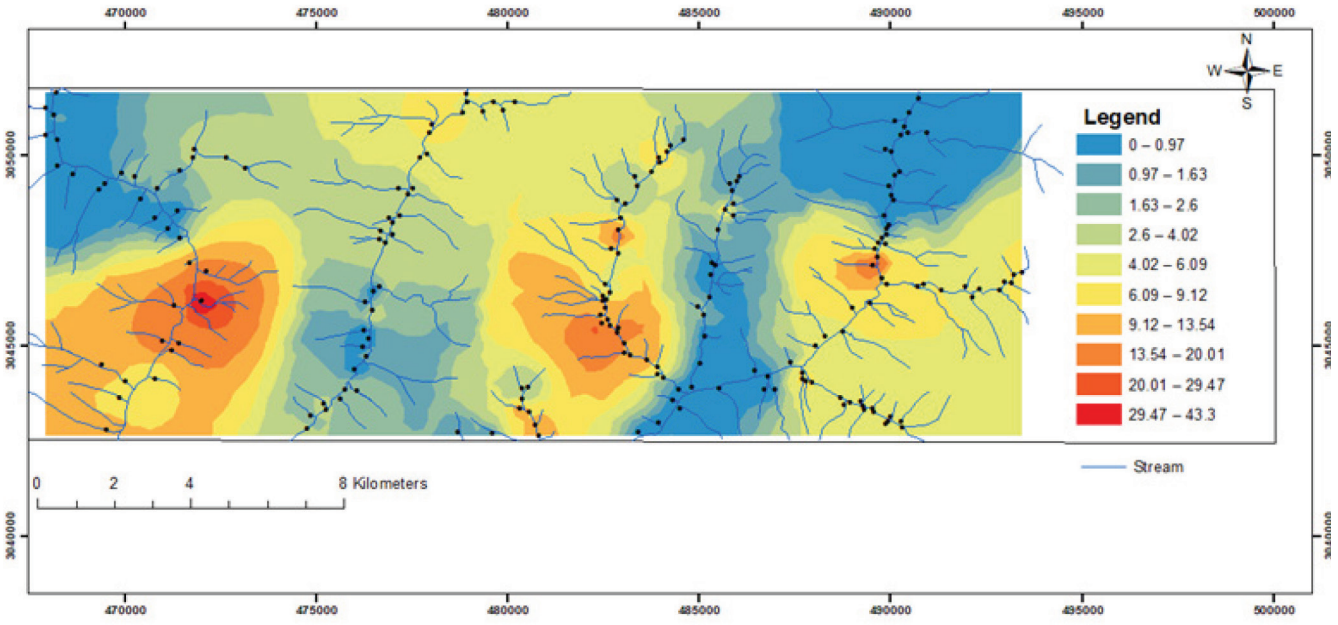

Fig. 9: Pb (ppm) distribution map of the study area.

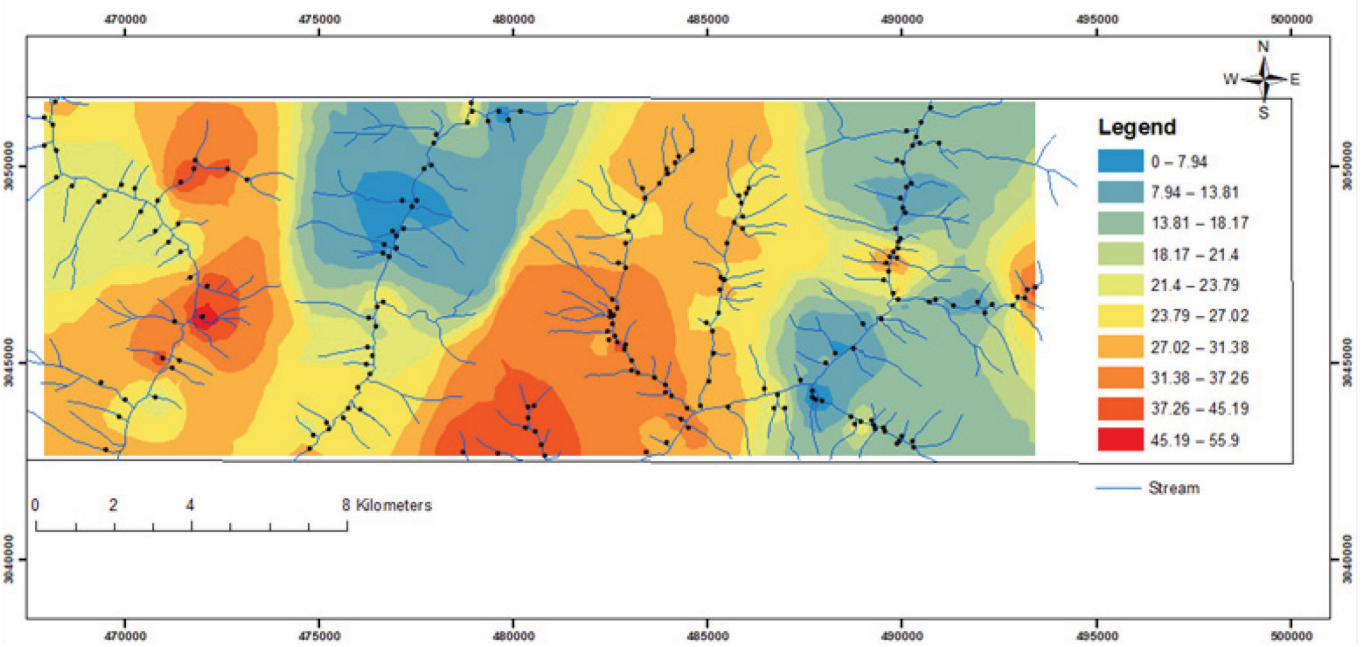

Fig. 10: Zn (ppm) distribution map of the study area.

DISCUSSION

Based on the geological condition of the area, the survey area is part of the LHS and GHS. The study area has been taken as a single window for threshold computation geostatistically since the terrain consists of schists and quartzites in LHS considering geological and lithological criteria for anomaly delineation (Reimann et al., 2005; Stanley and Sinclair, 1989). The Ulleri type orthogneiss, peralluminous, intruded within the Seti Formation has its origin within the plate in the upper crust possibly in a rift setting (Larsen, 2017). Based on geochemical data copper tends to be low concentration in orthogneiss (Fig. 8). Cu zones are not stratigraphically controlled (Figs. 8, 9, 10). The old working area of Wapsa has anomalous values for Cu, Pb, and Zn which is structurally a part of Dudh Koshi anticline (Figs. 8, 9, 10). Copper concentrations are located in the vicinity of orthogneiss within the Seti Formation represented by chloritic schists and quartzites (Figs. 3, 8). Benighat Slates has some erratic copper concentration (Fig. 8). Formation I has copper concentration rather than Pb and Zn (Fig. 8, 9, 10). The areas of low concentration can be eliminated rapidly as in central Nepal (UN/MEDP, 1981). The results of the threshold of Cu, Pb, and Zn are more or less compatible with central Nepal geochemical data (Table 3; UN/MEDP, 1981). The category matrix of the geochemical data has not been computed as in Dailekh and Achham (Khadka, 2003), as the results of Cu, Pb, and Zn are low concentration except in Wapsa area which was already explored for a copper prospect (Figs. 8, 9, 10). Drainage area and anomaly category from 1–4 can be established for this area whether it is suitable for follow-up recommendation or not, which are considered in Dailekh and Accham area geochemical survey (Khadka, 2003). The Benighat Slates carbonate rocks show erratic concentrations of Pb and Zn (Figs. 9, 10)**.** The IDW methods of interpolation using GIS is a viable option for anomaly detection of Cu, Pb and Zn as it estimates un-sampled locations by inverse distant squared weighting (IDW) (Figs. 8, 9, 10). However, Concentration (C-A) analysis was not carried out for anomaly delineation as followed by Hosaaeininasab et al. (2018).

CONCLUSION

The investigated area, geologically, is a part of the LHS and GHS. The LHS is represented by chloritic schists and quartzites of the Seti Formation intruded with Ulleri-type orthogneiss. Moreover, carbonaceous garnet schists, meta-sandstone, and carbonate beds of Benighat Slates overlie Seti Formation. Structurally, Dudhkoshi Anticline passes NW to SE in the west of Wapsa. The Main Central Thrust (MCT) separates the LHS and GHS in the upper parts of the Chheskam area (Table 1, Fig. 3). Since the pelitic protoliths are dominant over the survey area, the area is homogenous in terms of geology and mineralization except for the igneous protolith of Ulleri orthogneiss for geochemical data interpretation to detect anomalies.

The geochemical stream sediment survey shows that the Wapsa and Yasuka areas are significantly anomalous for Cu prospecting (Fig. 8). The Pb, and Zn concentrations are related to the vicinity of orthogneiss (Figs. 9, 10). The geostatistical analysis is an essential part of the data interpretation for base metal prospecting to identify thresholds and anomalies using log transformed data (UN/MEDP, 1981; Gałuszk, 2007; Hawkes and Webb, 1962; Reimann et al., 2005; Stanley and Sinclair, 1989). The IDW multivariate interpolation method is valid for natural sample anomaly detection (Figs. 8, 9, 10). There are no other cu anomalies except Wapsa and Yasuka to follow up and the same for Pb and Zn. The regional geochemical stream sediment survey is viable for base metal prospecting.

ACKNOWLEDGEMENTS

The author is thankful to the Director General Mr. Ram Prasad Ghimire of DMG for the support and consent given to use the database. Also equally thankful to the anonymous reviewer for suggestions to improve the manuscript.

REFERENCES

Amatya, K. M. and Jnawali, B. M., 1993, Geological map of Nepal, 1:1,000,000 scale. DMG Publication.

Arendt, J. W., 1978, Procedural manual for stream sediment reconnaissance sampling, DOE, USA, 53 p.

Barnes, J. W. and Lisle, R. J., 2004, *Basic geological mapping,* 4th edition, John Wiley and Sons Ltd., 198 p.

Bhandari, A. N., 1978, Drilling results of drill holes UNDDH-18, 19, 20 of Wapsa Khani, 72I/14, UN/MEDP unpublished report, DMG.

Brookfield, M. E., 1993, The Himalayan passive margin from Precambrian to Cretaceous times. Sedimentary Geology, v. 84, pp. 1–35.

Burg, J. P. and Chen, G. M., 1984, Tectonics and structural zonation of southern Tibet. China. Nature, v. 311, pp. 219–223.

Carranza, E. J. M., 2009, Geochemical anomaly and mineral prospectivity mapping in GIS, v.11, 347 p.

Chhetri, V. S., 1977, Report on the Channel sampling work in Wapsa Audit No. 6. DMG Unpublished report, 9. p.

Darnley, A. G., 1995, A global geochemical database for environmental resource management. UNESCO Publishing p.122.

DeCelles, P. G., Gehrels, G. E., Quade, J., and Ojha, T. P., 1998a, Eocene–early Miocene foreland basin development and the history of Himalayan thrusting, western and central Nepal. Tectonics, v. 17, pp. 741–765.

DeCelles, P. G., Gehrels, G. E., Quade, J., Ojha, T. P., Kapp, P. A., and Upreti, B. N., 1998b, Neogene foreland deposits, erosional unroofing, and the kinematic history of the Himalayan fold-thrust belt, western Nepal. Geological Society of America Bulletin, v. 110, pp. 2–21.

DeCelles, P. G., Robinson, D. M., Quade, J., Ojha, T. P., Garzione, C. N., Copeland, P., and Upreti, B. N., 2001, Stratigraphy, structure, and tectonic evolution of the Himalayan fold-thrust belt in western Nepal. Tectonics, 20, pp. 487–509.

DeCelles, P. G., Carrapa, B., Ojha, T. P., Gehrels, G. E., and Collins, D., 2020, Structural and Thermal evolution of the Himalaya Thrust Belt in Midwestern Nepal, GSA Special Paper, v. 547, pp. 1–77.

Dhital, M. R., 2015, *Geology of the Nepal Himalaya, Regional perspective of the classic collided orogeny.* Springer, 499 p.

Einfalt, H. C., Hoehndorf, A., and Kaphle, K. P., 1993, Radiometric age determination of the Dadeldhura granite, Lesser Himalaya, Far Western Nepal. Schweiz mineral petrogr Mitt. 73, pp. 97–106

Gaetani, M. and Garzanti, E., 1991, Multicyclic history of the Northern India continental margin (Northwestern Himalaya), AAPG Bull., 75, pp. 1427–1446.

Gałuszk, A., 2007, A review of geochemical background concepts and an example using data from Poland. Environ Geol., v. 52(5), pp. 861–870.

Gansser, A., 1964, *Geology of the Himalayas*. Wiley Interscience, London, 289 p.

Goscombe, B. and Hand, M., 2000, Contrasting P-T paths in the eastern Himalaya, Nepal: inverted isograds in a paired metamorphic mountain belt. Journal of Petrology, 41, pp. 1–47.

Goscombe, B., Gray, D., and Hand, M., 2006, Crustal architecture of the Himalayan metamorphic front in eastern Nepal. Gondwana Research 10, pp. 232–255.

Haldar, S., 2018, *Mineral exploration principles and applications.* Elsevier Inc., 370 p.

Hawkes, H. E. and Webb, J. S, 1962, Geochemistry in mineral exploration. Harper and Row, New York, 415 p.

Hodges, K. V., 2000, Tectonics of the Himalaya and southern Tibet from two perspectives. GSA Bulletin, v. 112(3), pp. 324–350.

Hoseininasab, M. and Daya, A. K., 2018, Separation of geochemical anomalies using inverse distant weighting (IDW) and concentration-area (C-A) fractal modeling based on stream sediments data in Janja Region, SE Iran. Bull. Min. Res. Exp., 156, pp. 167–178.

Ishida, T., 1969, Petrography and structure of the area between the Dudh Kosi and the Tama Kosi, east Nepal. Jour. Geol. Soc. Japan, v. 75, pp. 115–125.

Jessup, M. J., Law, R. D., Searle, M. P., and Hubbard, M., 2006, Structural evolution and vorticity of flow during extrusion and exhumation of the Greater Himalayan Slab, Mount Everest Massif, Tibet/Nepal: implications for orogen-scale flow partitioning. In: Law, R. D., Searle, M. P., and Godin, L. (eds.), Channel Flow, Ductile Extrusion and Exhumation in Continental Collision Zones. Geological Society London Special Publication, v. 268, pp. 379–413.

Jnawali, B. M. and Amatya, K. M., 1993, Application of Geochemical technique in exploration and evaluation of copper, lead and zinc resources of Nepal. Jour. of NGS, v. 9, pp. 8–20.

Joshi, P. R., Khan, H. R., Singh, S., Khadka, D. R., and Napit, D., 2004, Mineral Resources of Nepal. DMG Publication, 154 p.

Joshi, P. R. and Thapa, G. S., 1977, Report on Geological and geochemical investigation of mineral resources of a part of Dadeldhura granite massif, Dadeldhura district, Mahakali zone. DMG unpublished report, 23 p

Kaphle, K. P., 2020, Mineral resources of Nepal and their present status. www.ngs.org.np

Kaphle, K. P., 2011, Exploration results of iron ore deposit of Thoshe, Ramechhap, Nepal. Jour. Nepal Geol. Soc., v. 43, pp.153–166.

Kaphle, K. P. and Khan, H. R., 2006, Exploration and assessment of Thoshe iron deposit in Ramechhap district, Central Nepal. DMG annual report no.3, pp. 9–24.

Kaphle, K. P. and Khan, H. R., 1994, Geological report on geochemical reconnaissance and preliminary follow up investigation of gold, uranium and base metals in some part of Bajhang and Baitadi districts, far-western Nepal. DMG unpublished report 33 p.

Kaphle, K. P. and Khan, H. R., 1993, Reconnaissance and preliminary follow up investigation of gold, uranium and base metals in Chamliya River and its catchment areas in Baitadi and Darchula districts, far-western Nepal. DMG unpublished report, 39 p.

Kaphle, K. P., 1992, Geology, petrology and geochemistry of Dadeldhura granite massif, far western Nepal. Kashmir Jour. Geology, v. 10, pp. 75–92.

Kaphle, K. P., 1982, Geological and geochemical exploration of copper-tungsten prospect of Bamangaon and adjacent areas, Dadeldhura district, far-western Nepal. Tungsten geology Proceedings, Jiangxi, China, pp. 123–126.

Kaphle, K. P., Joshi, P. R, and Khan, H. R., 1996, Placer gold occurrences in the major rivers of Nepal and their possible primary source. Jour. Nepal Geol. Soc., v.13, pp. 51–64.

Kaphle, K. P. and Khadka, D. R., 2005, Preliminary follow up gold exploration along Kaligandaki valley, in some parts of Myagdi, Parbat and Baglung districts, western Nepal, DMG annual report No. 2, pp. 6–15.

Khadka, D. R., 2003, Geochemical prospecting of base metals and gold in parts of Dailekh and Achham districts, Mid-Western Nepal. DMG Annual Report, v. 1, pp. 72–76.

Khan, H. R., 1994, Reconnaissance geochemical survey and preliminary follow up investigation for Gold, uranium and base metals in a part of Baitadi and Bajhang districts, far-western Nepal. DMG unpublished report, 19 p.

Khan, H. R., 1995, Reconnaissance geochemical survey for Gold, uranium and base metals in a part of Bajhang district, Far-Western Nepal. DMG unpublished report, 18 p.

Khan, H. R., 1997, Follow-up geochemical exploration for base metals in Bauligad, Kucha, Dilgad, Saingad, Tamoli, and Sheri

areas, Bajhang district, Far-Western Nepal. DMG unpublished report, 21 p.

Kohn, M. J., Paul, S. K., and Corrie, S. L., 2010, The lower Lesser Himalayan sequence: a Paleoproterozoic arc on the northern margin of the Indian plate. Geological Society of America Bulletin 122, 323e335, http://dx.doi.org/10.1130/B26587.1.

Larson, K. P. and Godin, L., 2009, Kinematics of the Greater Himalayan sequence, Dhaulagiri Himal: implications for the structural framework of central Nepal. Journal of the Geological Society, London 166, pp. 25–43.

Larson, K., Cottle, J., Lederer, G., and Rai, S. M., 2017, Defining shear zone boundaries using fabric intensity gradients: An example from the east central Nepal Himalaya. Geosphere, 13, pp. 771–781.

Larson, K. P., Kellett, D. A., Cottle, J. M., King, J., Lederer, G., and Rai, S. M., 2016, Anatexis, cooling, and kinematics during orogenesis: Miocene development of the Himalayan metamorphic core, east-central Nepal. Geosphere, 12, pp. 1575–1595.

Larson, K. P., Cottle, J. M., Lederer, G., and Rai, S. M., 2017, Defining shear zone boundaries using fabric intensity gradients: an example from the East-Central Nepal Himalaya. Geosphere, 13. http://dx.doi.org/10.1130/GES01373.1.

Larson, K., Piercey, S., and Cottle, J., 2019, Preservation of a Paleoproterozoic rifted margin in the Himalaya: Insight from the Ulleri-Phaplu-Melung orthogneiss. Geoscience Frontiers, 10, pp. 873–883.

Le Fort, P., 1975, Himalayas: The collided range. Present knowledge of the continental arc. American Journal of Science, v. 275-A, pp. 1–44.

Le Fort, P. and Rai, S. M., 1999, Pre-tertiary felsic magmatism of the Nepal Himalaya: recycling of continental crust. Journal of Asian Earth Sciences, 17, pp. 607–628.

Liu, S., Zhang, G., Zhang, L., Wang, S., Upreti, B.N., Adhikari, D. P., Wu, C., and Wang, J., 2022, Diverse anatexis in the Main Central Thrust Zone, Eastern Nepal: Implications for melt evolution and exhumation process of the Himalaya. Journal of Petrology, v. 63(3), pp. 1–26.

Martin, A. J., 2016, A review of definitions of the Himalayan Main Central thrust. International Journal of Earth Sciences, pp. 1–15.

Martin, A. J., DeCelles, P. G., and Gehrels, G. E., 2005, Isotopic and structural constraints on the location of the Main Central thrust in the Annapurna range, central Nepal Himalaya. Bulletin of the Geological Society of America, 117, pp. 926–944.

Martin, A. J., 2017, A review of Himalayan stratigraphy, magnetism and Structure. Gondwana Research, v. 49, pp. 42–80.

Mitchel, A. H. G., 1981, Himalayan and Transhimalayan granitic rocks in and adjacent to Nepal and their mineral potential. Jour. Nepal Geol. Soc., v. 1(1), pp. 41–52.

NERC, 2001, BGS, Mineral exploration methods in Britain. Panned concentrate draining sampling, 2 p.

NERC, 2000, BGS, Mineral exploration methods in Britain. Stream sediment sampling, 2 p.

Parrish, R. R. and Hodges, K. V., 1996, Isotopic constraints on the age and provenance of the Lesser and Greater Himalayan sequences, Nepalese Himalaya. Geological Society of America Bulletin, v. 108, pp. 904–911.

Paudel, L. P. and Arita, K., 2000, Tectonic and polymetamorphic history of the Lesser Himalaya in Central Nepal. Jour. Asian Earth Science, v. 18, pp. 561–584.

Pearson, O. N. and DeCelles, P. G., 2005, Structural geology and regional tectonic significance of the Ramgarh thrust, Himalayan fold-thrust belt of Nepal. Tectonics, 24. http://dx.doi.org/10.1029/2003TC001617.

Ranjitkar, S. B., 1976, Report on mineral economics of Wapsa Khani. Unpublished report, Department of Mines and Geology (DMG), 6 p.

Reimann, C., Filzmoser, P., and Garrett, R.G., 2005, Background and threshold, critical comparison of methods of determination. Sci. Total Environ., 346, pp. 1–16.

Sakai, H., 1983, Geology of the Tansen Group of the Lesser Himalaya in Nepal. Mem. Fac. Sci. Kyushu Univ. Ser D Geol., v. 25(1), pp. 27–74.

Sakai, H., Iwano, H., Danhara, T., Takigami, Y., Rai, S. M., Upreti, B. N., and Hirata, T., 2013, Rift related origin of the Paleoproterozoic Kuncha Formation, and cooling history of the Kuncha nappe and Taplejung granites, eastern Nepal Lesser Himalaya: a multichronological approach. Island Arc, 22, pp. 338–360.

Schelling, D., 1992, The Tectonostratigraphy and structure of the eastern Nepal Himalaya. Tectonics, 11, pp. 925–943.

Shrestha, N. R. and Bajracharya, R. B., 1979, Report on IP and magnetic survey of part of Wapsa copper prospect, Solukhumbu District, Unpublished report, DMG.

Shrestha, P. L., 1980, Report on second phase Wapsa drilling, unpublished report, DMG.

Shrestha, S. B. and Shrestha, J. N., 1984, Geological map of Eastern Nepal. Scale: 1:250,000. Department of Mines and Geology, Kathmandu.

Shepard, D., 1968, A two-dimensional interpolation function for irregularly-spaced data. Proceedings of the 1968, ACM National Conference, pp. 517–524.

Sinclair, A. J., 1974, Selection of threshold values in geochemical data using probability graphs. Journal of Geochemical Exploration, 3, pp. 129–149.

Stanley, C. R. and Sinclair, A. J., 1989, Comparison of probability plots and gap statistics in the selection of threshold for exploration geochemistry data. Jour. Geochemical Exploration, 32, pp. 355–357.

Stöcklin, J., 1980, Geology of Nepal and its regional frame: Geological Society London Journal, v. 137, pp. 1–34.

Talalov, V. A., 1972, Geology and ores of Nepal. Nepal Geological Survey/DMG, v. 2, Unpublished report, 483 p.

UN/MEDP, 1981, Mineral exploration results in a part of Nepal, Technical report, 196 p.

UN/ESCAP with DMG, 1993**,** Atlas of Mineral Resources of the ESCAP Region, Geology and Mineral Resources of Nepal, v. 9, 107 p.

Upreti, B. N. and Le Fort, P., 1999. Lesser Himalayan crystalline nappes of Nepal: Problems of their origin. Geological Society of America Special Paper, 328, pp. 225–238.

Valdiya, K. S., 1980, Geology of the Kumaun Lesser Himalaya: Dehra Dun, Wadia Institute of Himalayan Geology, 291 p.

Zheng, Y., Sun, X., Gao, S., Wang, C., Zhao, Z., Wu, S., Li, J., and Wu, X., 2014, Analysis of stream sediment data for exploring the Zhou porphyry Cu deposit, southern Tibet. Journal of Geochemical Exploration, v. 143, pp. 19–30.